Tellus (1993), 45A, 159–167
Printed in Belgium – all rights reserved

TELLUS
ISSN 0280–6495

The influence of tropospheric static stability on upper-level frontogenesis

By MARCEL SAUTE, *Université Blaise Pascal, Laboratoire de Météorologie Physique, URA CNRS D0267, 24, Avenue des Landais, 63177 Aubiere Cedex, France*

(Manuscript received 2 July 1992; in final form 6 November 1992)

ABSTRACT

Upper-level frontogenesis in an inviscid, dry and adiabatic fluid forced by confluence is investigated by means of a two-dimensional semi-geostrophic model using the specific volume as an isentropic vertical coordinate. The initial conditions are specified given an analytical continuous potential vorticity field in the presence of a temperature contrast at the ground, the lower boundary condition requiring an appropriate treatment because the ground intersects the first levels of the model. The paper has concentrated on the rôle of the horizontal variations of low and middle tropospheric potential vorticity in the intensification of the upper-level jet-front system. Destabilization of the cold air mass relative to the warm air mass yields an appreciable increase of the strength of the upper-level jet. Several meteorological situations characterized by such variations of static stabilities have been described elsewhere.

1. Introduction

Much theoretical work has been done using the geostrophic momentum approximation on some idealized atmospheric states to study surface as well as upper-level frontogenesis. From the work of Hoskins and Bretherton (1972), Ertel potential vorticity (*PV*) appeared as the key ingredient of a semi-geostrophic description of frontogenesis. In the earliest models (Hoskins,1971), frontogenesis occurred in a constant *PV* fluid and in a two-layer fluid. Further idealized *PV* fields taking into account the presence of a deformable tropopause, the continuity of *PV* distribution between troposphere and stratosphere and ground-surface temperature contrasts, were proposed to obtain more realistic descriptions of upper-level frontogenesis. Restricting ourselves to two-dimensional dry frontogenesis, it appears that pure confluence models (Hoskins, 1971; Hoskins and Bretherton, 1972; Gidel and Shapiro, 1979; Buzzi et al., 1981; Moore, 1987), characterized by large-scale time-independent height-independent hyperbolic deformation flow, yield moderate upper-level fronts and a direct circulation in the neighborhood. Moore (1987) showed that the inclusion of an appropriate localized perturbation in the region of the jet results in the intensification of the upper-level front. Recently, Fulton and Schubert (1991), using an isentropic coordinate model, produced a quite realistic upper-level front as well as the beginning of tropopause folding. In a second class of models, referred to as horizontal shear models, the large scale forcing proceeds by means of the vertical component of vorticity rotating the along-front temperature gradient. Using a hierarchy of numerical models, Reeder and Keyser (1988) showed that, in the presence of a strong shear, either the anelastic approximation or the geostrophic momentum approximation models lead to reinforced upper-level fronts and locate the maximum of subsidence in the neighborhood of the upper-level front on the warm side of the vorticity maximum. These results are in agreement with the arguments developed by Shapiro (1981). The same conclusions were drawn from a primitive equation model by Keyser and Pecnick (1985).

In this paper, we shall consider the frontal zone resulting from a continuous distribution of potential vorticity, including a variable depth of the tropopause and a surface temperature gradient on the ground, here assumed horizontal. We shall be

interested in the influence of horizontal gradients of tropospheric static stability and then of $P\dot{V}$ at the interface between air masses on the strength of the upper-level jet. Thorpe (1990) investigated frontogenesis at the interface of two air masses of different but constant PV, noting that a number of meteorological situations exhibit such horizontal variations of tropospheric PV. Some observational aspects were previously described by Bosart (1975) and Shapiro et al. (1987).

We use an isentropic α-coordinate model, as did Buzzi et al. (1981), for which the PV conservation law is particularly simple. It is one of the advantages choosing this vertical coordinate, despite the difficulty encountered in inverting the PV field to obtain the geostrophic streamfunction. Another difficulty is related to the lower boundary condition, since the ground may intersect the levels of the model. Necessary details will appear in the following.

It is worthwhile mentioning that potential temperature and more generally isentropic coordinates are particularly convenient for resolving fronts. From the work of Sanders (1955), horizontal potential temperature gradient was used to diagnose surface fronts. Horizontal wet-bulb potential temperature gradient may be preferred now, either in objective analysis (Uccellini and Johnson, 1979; Sanders and Bosart, 1985; Hoinka et al., 1990; Saarakivi and Puhakka, 1990), or in non-isentropic coordinate numerical models (Baldwin et al., 1984; Knight and Hobbs, 1988; Sortais, 1991). Petterssen (1936, 1956) defined atmospheric frontogenesis as the temporal rate of change along a parcel trajectory of the magnitude of the horizontal potential temperature gradient. This function was recently generalized as a vector frontogenesis function by Keyser et al. (1988). From Reed (1955), it was recognized that upper-level fronts were more readily resolved with conventional radiosonde data when viewed from an isentropic perspective, thus motivating subsequent efforts in objective analysis and numerical modeling in isentropic coordinates. An excellent review about the advantages and disadvantages of isentropic coordinates is given in Hsu and Anthes (1990).

Section 2 describes the semi-geostrophic equations and the appropriate boundary conditions. In Section 3 is defined the initial analytical potential vorticity field and the associated temperature variations on the lower boundary. Detailed results are presented in Section 4 and concluding remarks in Section 5.

2. The description of the model

We shall consider frontal zones that are the result of a geostrophic stretching deformation field. For the case of an incompressible fluid treated here, we use an isentropic coordinate system, for which the vertical coordinate is the specific volume α which is thus a conservative quantity. The cross-front x-axis points towards the warmer air.

Assuming f constant, it is easy to restrict the primitive equations of motion to the two-dimensional case in which there is cross-front geostrophic balance

$$fv = \frac{\partial M}{\partial x}, \tag{1}$$

$$\frac{\partial v}{\partial t} + (u_g + u_{ag})\frac{\partial v}{\partial x} + v\frac{\partial v}{\partial y} + fu_{ag} = 0, \tag{2}$$

$$\frac{\partial M}{\partial \alpha} = p, \tag{3}$$

$$\frac{\partial}{\partial t}\left(\frac{\partial p}{\partial \alpha}\right) + V_g \cdot \nabla \frac{\partial p}{\partial \alpha} + \frac{\partial}{\partial x}\left(u_{ag}\frac{\partial p}{\partial \alpha}\right) = 0. \tag{4}$$

These equations are as in Buzzi et al. (1981), the streamfunction M being defined as

$$M = \alpha p + gz, \tag{5}$$

g and ag subscripts identifying the geostrophic and ageostrophic components of the wind and all other quantities using standard notation.

To these equations, we add the conservation equation for α

$$\frac{D\alpha}{Dt} = 0, \tag{6}$$

with

$$\frac{D}{Dt} = \frac{\partial}{\partial t} + (u_g + u_{ag})\frac{\partial}{\partial x} + v\frac{\partial}{\partial y},$$

meaning that trajectories will be along α-coordinate lines, and the conservation equation for the

potential vorticity Q, following parcel trajectories of a fluid which is inviscid and adiabatic,

$$\frac{DQ}{Dt}=0, \tag{7}$$

with

$$Q=-\left(f+f^{-1}\frac{\partial^2 M}{\partial x^2}\right)\left(\frac{\partial^2 M}{\partial \alpha^2}\right)^{-1}.$$

The geostrophic stretching deformation field here assumed to be independent of time and height will be represented by

$$u_d=-kx,$$

$$v_d=ky,$$

where $k=10^{-5}\,s^{-1}$ ($k/f\approx 0.1$ according to Hoskins and Bretherton, 1972).

The solution of our system of equations and then the formation of the frontal zone will be described by

$$U=u_d+u(x,\alpha,t),$$

$$V=v_d+v(x,\alpha,t).$$

An appropriate representation of $u(x,\alpha,t)$ allows us to get rid of the y-dependence of the foregoing equations, which become

$$fv=\frac{\partial M}{\partial x}, \tag{8}$$

$$\frac{\partial v}{\partial t}-kx\frac{\partial M}{\partial x}+kv+u_{ag}\left(f+\frac{\partial v}{\partial x}\right)=0, \tag{9}$$

$$\frac{\partial M}{\partial \alpha}=p, \tag{10}$$

$$\frac{\partial}{\partial t}\left(\frac{\partial p}{\partial \alpha}\right)-kx\frac{\partial}{\partial x}\left(\frac{\partial p}{\partial \alpha}\right)+\frac{\partial}{\partial x}\left(u_{ag}\frac{\partial p}{\partial \alpha}\right)=0. \tag{11}$$

Using the horizontal geostrophic coordinate of Hoskins

$$X=x+v/f,$$

the corresponding geostrophic streamfunction becomes

$$\Phi=\alpha p+gz+v^2/2. \tag{12}$$

Transformation of eq. (9) or Kelvin's theorem gives (Hoskins and Bretherton, 1972)

$$\frac{DX}{Dt}=-kX, \tag{13}$$

$$X(t)=X(t=0)\exp(-kt), \tag{14}$$

t being only a parameter, making implicit the time integration. This means that, Q being conserved, if $(X(0),\alpha)$ is the initial position of a given particle, then

$$(X(t),\alpha)=(X(0)\exp(-kt),\alpha)$$

is its final position at time t, and

$$Q(X,\alpha,t)=Q(X(0),\alpha,t=0), \tag{15}$$

where

$$f^2\frac{\partial^2\Phi}{\partial\alpha^2}-\frac{\partial^2\Phi}{\partial\alpha^2}\frac{\partial^2\Phi}{\partial X^2}+\left(\frac{\partial^2\Phi}{\partial\alpha\,\partial X}\right)^2=-f^3/Q. \tag{16}$$

The model solution concerning the along-front circulation is obtained at any time t, by means of Kleinschmidt's invertibility principle, applied to the Monge-Ampère type eq. (16), which may be regarded as elliptic when Q is positive. The integration procedure will be given below. The velocity v parallel to the front and other variables may then be deduced from the streamfunction Φ.

Boundary conditions appropriate to solving eq. (16) are the following. The top of the model is situated in the lower stratosphere at a constant pressure p_T, where $\alpha=\alpha_T$, thus

$$\frac{\partial\Phi}{\partial\alpha}=p_T. \tag{17}$$

On the lateral boundaries, the domain of integration being sufficiently wide, we have

$$\frac{\partial\Phi}{\partial X}\to 0 \quad \text{as} \quad |X|\to\infty. \tag{18}$$

The situation is a little more complex on the lower boundary. We must take account of a temperature gradient at the ground which, in this paper, has been assumed horizontal, $z_s=0$. Our approach is to define the ground as

$$\alpha_s=\alpha_s(X), \tag{19}$$

(s-subscript denoting the α level of the ground) at $t=0$, with $\partial\alpha_s/\partial X>0$ for a cold front. Making use of the α-conservation law, particles which are on the ground will remain there, so that

$$\frac{D\alpha_s}{Dt}=0. \tag{20}$$

Then we shall write that on the ground

$$\Phi_s=\alpha_s p_s+v_s^2/2. \tag{21}$$

An appropriate transformation allows us to write eq. (21) as an equation on the geostrophic streamfunction Φ_0 evaluated on the virtual level α_0. The last equation has to be solved by iteration.

3. The initial state

Every numerical simulation reported below was initialized with an analytical potential vorticity field describing two air masses, each characterized by a number of parameters. The vertical profile of Q is determined according to the following relations,

$$Q(\alpha)=A\alpha^2+C+B\alpha\,\mathrm{th}\,\frac{\alpha-\alpha_\tau}{\delta}$$

$$\text{if}\quad \alpha\leqslant\alpha_\tau, \tag{22a}$$

$$Q(\alpha)=D\alpha+E+B\alpha\,\mathrm{th}\,\frac{\alpha-\alpha_\tau}{\delta}$$

$$\text{if}\quad \alpha>\alpha_\tau. \tag{22b}$$

The above linear function of α is simply the derivative of the quadratic one at $\alpha=\alpha_\tau$. For any X, the remaining five parameters A, B, C, α_τ and δ are not independent and must satisfy a number of requirements (i) $Q(\alpha)$ is everywhere positive, (ii) $\partial\theta/\partial\alpha$ is always positive, (iii) the top pressure is $p_T=140$ hPa. Clearly, A represents the static stability of the troposphere, B the Q-variation amplitude across the tropopause, α_τ the height of the tropopause and δ the steepness of the variation of Q across the tropopause. The additional parameter C is necessary to make Q positive in the lower troposphere.

The specification of the temperature gradient at the ground obeys the following relation

$$\alpha_s(X)=\alpha_0+\Delta\alpha(1+\mathrm{th}(X/L_s)), \tag{23}$$

α_0 being the lowest level of the model. The temperature contrast is

$$\Delta T=2\,\Delta\alpha p_s/R,$$

(R gas constant for dry air), assuming that, at $t=0$, we have $p_s=1000$ hPa, for any value of X. In the following, $\Delta T=37°$ everywhere.

It is useful to consider that, at a large distance from the central part of the domain, only the first term of eq. (16) is essential, $Q\propto\partial^2\Phi/\partial\alpha^2=\partial p/\partial\alpha$. From this point of view, comparing our model with a Z vertical coordinate semi-geostrophic model (e.g., Moore, 1987), the following quantities play the same role outside the central region.

α-coordinate model	Z-coordinate model
$p\propto\partial\Phi/\partial\alpha$	$\vartheta\propto\partial\Phi/\partial Z$
$Q\propto(\partial p/\partial\alpha)^{-1}$	$Q\propto\partial\vartheta/\partial Z$.

4. Results

A number of numerical simulations were performed to study the ability of our model to produce realistic dry upper-level and surface jets from given potential vorticity fields.

The domain is rectangular, ranging from -2000 km to 2000 km in X, from $\alpha_0=0.7492\ \mathrm{m^3\,kg^{-1}}$ to $\alpha_T=4.5295\ \mathrm{m^3\,kg^{-1}}$ in α. The grid spacings are $\Delta X=50$ km and $\Delta\alpha=0.1575\ \mathrm{m^3\,kg^{-1}}$, i.e., 81 points in the horizontal and 25 points in the vertical. As explained before, the parameters defining the initial PV field are adjusted so that, given the surface temperature contrast, the pressure p_T at the top of the domain is constant. Fig. 1 exhibits a typical initial Q-field in (X,α) space.

For any simulation, eq. (16) was solved using a multigrid algorithm, taking advantage that, as explained in Fulton et al. (1986) , the slow convergence of the Gauss-Seidel relaxation scheme is due to the lowest wavenumber modes. These modes may be approximated on a coarser grid with much less work. Consequently, three coarser grids were defined, namely grid G1, 11×4 points, G2, 21×7 points and G3, 41×13 points. On each of these grids, the solution of eq. (16), obtained by means of a non linear relaxation scheme, is used as a first guess on the next finer grid and so on. The

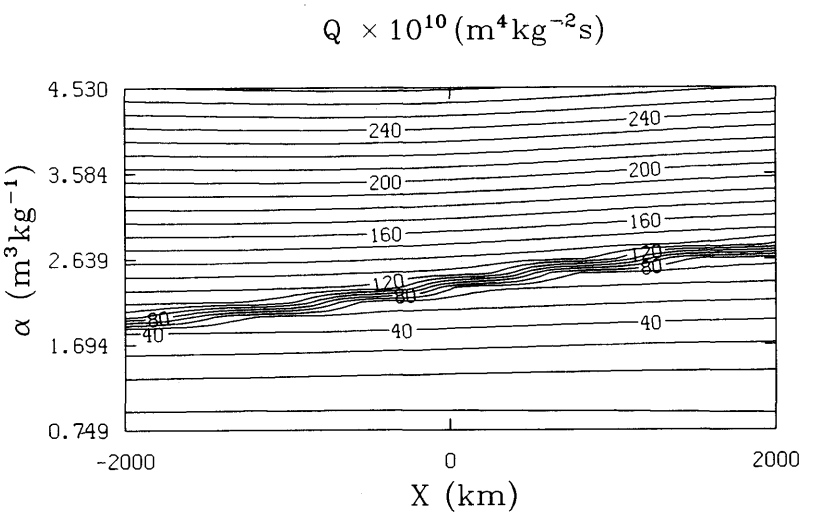

Fig. 1. The initial Q field in (X, α) space. This field leads to Q, v, p and θ fields of Fig. 2 after contraction.

discretization of the last two terms of the first member of eq. (16) was accomplished using a nine-point system analogous to that of Miyakoda (1960). This choice is time-consuming, but guarantees an adequate representation of this non-linear operator.

Finally, boundary conditions on the lowest level of the model are satisfied by an iterative procedure. Due to the vertical resolution of the model and the value of the surface temperature contrast, the earth's surface, defined by $\alpha_s(X)$, does not intersect any level, the first one being a completely virtual level as mentionned before.

In the following, we shall particularly examine how the relative variations of the initial tropospheric static stabilities of the two air masses influence the strength of the upper-level jet. Only the static stability of the troposphere is affected by the A parameter variations. Fig. 2 shows cross-sections of Q, v, p and θ at $t = 60$ h. Part (a) shows the Q field in the working (X, α) space, in units of 10^{-10} m^4 kg^{-2} s, part (b) shows the v and p fields in (X, α) space, i.e., the rough results of integration of (16), and part (c) shows the v and θ fields in the physical space (x, p) after transformation from geostrophic to physical abscissae. In this first case, the tropospheric static stabilities of the air masses are not very different. The same fields appear on Fig. 3, in a second case where the tropospheric static stabilities are rather different on both sides of the front.

In either case, the model develops well-separated upper and lower-level jet-front systems. The upper-level is always slightly stronger than the lower-level one, in agreement with the results of Fulton and Schubert (1991). Moore (1987), investigating a continuously varying PV fluid by means of a two-dimensional Z-coordinate model, attributed the relative weakness of the upper-level front as compared to the surface one to the Boussinesq hypothesis and the height-independency of the deformation field. However, Reeder and Keyser (1988) obtained the result that the jet-fronts deriving from the geostrophic momentum approximation are virtually indistinguishable from that derived from the anelastic approximation, in the case of zero or weak horizontal shear.

Returning to our results, it is true that the α-coordinate, as with the θ coordinate, is more appropriate, even with a moderate resolution, to represent the upper troposphere and the lower stratosphere, in spite of the difficulties linked with the lower boundary. It is in particular easier to model realistic variations of the potential vorticity across the tropopause, varying parameters B and δ of eq. (22).

It is important to realize that if the high values

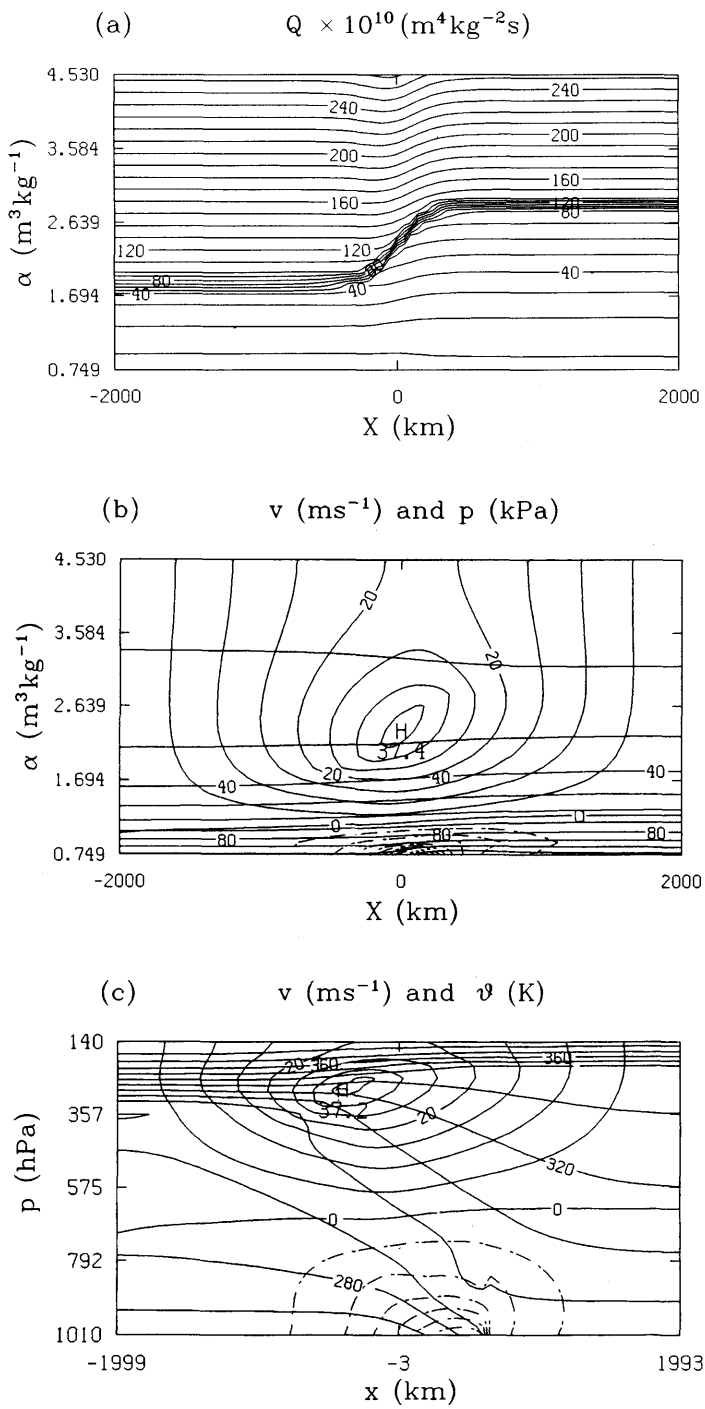

Fig. 2. Structure of the front at $t = 60$ h. The initial tropospheric static stabilities of both air masses are comparable. (a) Q in (X, α) space, (b) v and p in (X, α) space, (c) v and θ in the physical space (x, p).

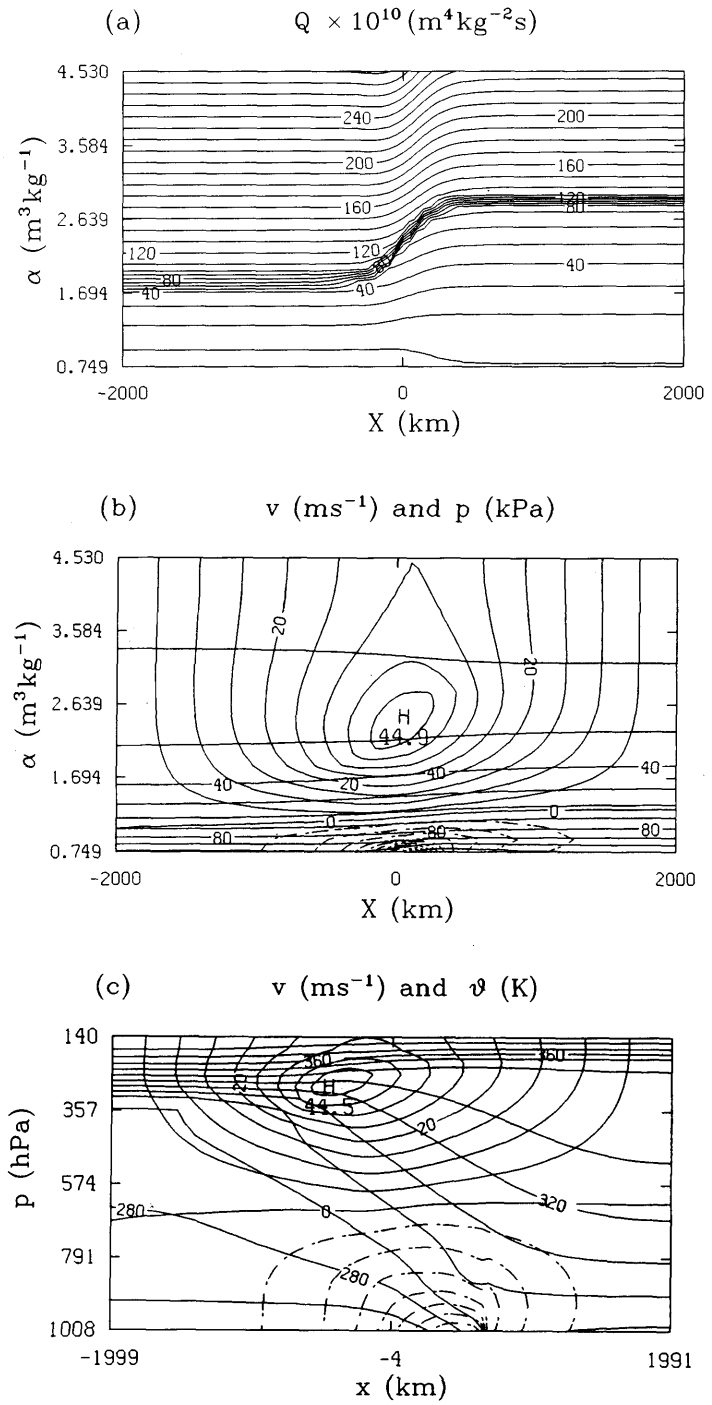

Fig. 3. Same as in Fig. 2. The initial tropospheric static stability of the cold air mass has decreased, that of the warm air mass has increased.

of potential vorticity Q ($\propto(\partial p/\partial\alpha)^{-1}$ far from the center) undergo some relative variations, even of some importance, the degree of stability of the lower stratosphere and the upper troposphere is not altered. In contrast, the stability of the lower and middle troposphere is very sensitive to the same variations of weaker values of Q. This sensitivity is illustrated in Fig. 3. It is apparent, going from Fig. 2c to 3c, that cold air has become less stable and warm air more stable. In other terms, it means (see Figs. 2a and 3a) that the mean tropospheric PV for cold air has decreased, while the mean tropospheric PV for warm air has increased, i.e., finally $\bar{Q}_{\text{cold}} \leqslant \bar{Q}_{\text{warm}}$ for the troposphere. The intensification of the upper-level jet results, as well as that of the cross-front velocity gradient on the cyclonic side of the jet. We may conclude that increasing the horizontal gradient of initial tropospheric PV (x-axis from cold to warm air) yields an appreciable intensification of the upper-level jet. Our results particularize those of Thorpe (1990) who deduced, from purely geometrical arguments, that, given two air masses characterized by constant but different PV values, upper-level frontogenesis is favoured when the horizontal gradient of PV is directed from cold to warm air. It is worth mentioning that in both cases (Figs. 2, 3), the vertically averaged PV from the ground to the top of the model is in fact always larger for cold air, although the opposite is true in the lower part of the model. It would be necessary to get rid of the assumption $\theta = \text{constant}$ at the top of the model to reverse the sense of the above overall horizontal gradient of PV.

Concerning the vertical gradient of PV across the tropopause, it depends on the steepness parameter δ, but also on B-values representative of the overall variation of PV in that zone. Fig. 2a (or 3a) is obtained with a common value $\delta = 0.05\ \text{m}^3\ \text{kg}^{-1}$ for cold and warm air masses, but different B values. No systematic study was carried out to investigate the sensitivity of the upper-level front to variations of the above defined parameters. However, dividing δ for the cold air mass by a factor 5, we obtain a vertical gradient of PV of an approximately uniform value on either side of the front. As expected, the upper-level jet is enhanced, only by 1 m/s in this experiment, as well as the cold side cross-front velocity gradient. Indeed, increasing the steepness of the Q-variation across the tropopause, on either side or not, strengthens slightly the upper-level front. However, it is rather uncertain to define realistic δ-values from the available data, either from radiosonde or from stratosphere-troposphere radar experiments.

5. Conclusion

The present study was concerned with a simple model of frontogenesis to investigate the role of horizontal variations of tropospheric potential vorticity, in other terms of static stability between two air masses across the front. The model involved simultaneous use of geostrophic and α-isentropic coordinates, the last one being most appropriate to study upper-level frontogenesis. Initialization was accomplished by means of an analytical potential vorticity field describing rather realistically both air masses forced by confluence, in the presence of a temperature contrast at the ground.

Previous results of Thorpe (1990), according to which upper-level frontogenesis is favoured in the case where the initial constant PV of the cold air mass is less than that of the warm air mass, are particularized in the sense that even if the horizontal gradient of the mean vertically averaged PV is negative (from warm to cold), the creation of a positive, then reverse, horizontal gradient of PV in the middle and lower troposphere is sufficient to yield a substantial enhancement of the upper-level jet and the corresponding cross-front velocity gradient.

The top of our model was defined in terms of pressure, which is kept constant, and corresponds to $\theta = \text{constant}$. It is possible to remove this condition, in which case the top and bottom boundaries will both intersect the levels of the model, but it appeared that our treatment overcame these difficulties. It is then a way to define even more realistic potential vorticity fields. An important remaining problem is how to quantify the PV changes produced by various physical processes.

REFERENCES

Baldwin, D., Hsie, E.-Y. and Anthes, R. A. 1984. Diagnostic studies of a two-dimensional simulation of frontogenesis in a moist atmosphere. *J. Atmos. Sci. 41*, 2686–2700.

Bosart, L. F. 1975. New England frontogenesis. *Q. J. R. Meteorol. Soc. 101*, 957–978.

Buzzi, A., Trevisan, A. and Salustri, G. 1981. Internal frontogenesis: a two-dimensional model in isentropic semi-geostrophic coordinates. *Mon. Wea. Rev. 109*, 1053–1060.

Fulton, S. R., Ciesielski, P. E. and Schubert, W. H. 1986. Multigrid Methods for Elliptic Problems: A Review. *Mon. Wea. Rev. 114*, 943–959.

Fulton, S. R. and Schubert, W. H. 1991. Surface frontogenesis in isentropic coordinates. *J. Atmos. Sci. 48*, 2534–2541.

Gidel, L. T. and Shapiro, M. A. 1979. The role of clear air turbulence in the production of potential vorticity in the vicinity of upper tropospheric jet stream-frontal systems. *J. Atmos. Sci. 36*, 2125–2138.

Hoinka, K. P., Hagen, M., Volkert, H. and Heimann, D. 1990. On the influence of the Alps on a cold front. *Tellus 42A*, 140–164.

Hoskins, B. J. 1971. Atmospheric frontogenesis: some solutions. *Q. J. R. Meteorol. Soc. 97*, 139–153.

Hoskins, B. J. and Bretherton, F. P. 1972. Atmospheric frontogenesis models: mathematical formulation and solution. *J. Atmos. Sci. 29*, 11–37.

Hsu, Y.-J. and Arakawa, A. 1990. Numerical modeling of the atmosphere with an isentropic vertical coordinate. *Mon. Wea. Rev. 118*, 1933–1959.

Keyser, D. and Pecnick, M. J. 1985. A two-dimensional primitive equation model of frontogenesis forced by confluence and horizontal shear. *J. Atmos. Sci. 42*, 1259–1282.

Keyser, D., Reeder, M. J. and Reed, R. J. 1988. A generalization of Petterssen's frontogenesis function and its relation to the forcing of vertical motion. *Mon. Wea. Rev. 116*, 762–780.

Knight, D. J. and Hobbs, P. V. 1988. The mesoscale and microscale structure and organization of clouds and precipitation in midlatitude cyclones. Part XV: A numerical modeling study of frontogenesis and cold-frontal rainbands. *J. Atmos. Sci. 45*, 915–930.

Miyakoda, K. 1960. Numerical solution of the balance equation. Technical report of the Japan Meteorological Agency. No. 3, 15–34.

Moore, G. W. K. 1987. Frontogenesis in a continuously varying potential vorticity fluid. *J. Atmos. Sci. 44*, 761–770.

Petterssen, S. 1936. Contribution to the theory of frontogenesis. *Geofys. Publ. 11*, 1–27.

Petterssen, S. 1956. *Weather analysis and forecasting, Vol. 1, Motion and motion systems.* 2nd edition McGraw-Hill, 428 pp.

Reed, R. J. 1955. A study of a characteristic type of upper-level frontogenesis. *J. Meteor. 12*, 226–237.

Reeder, M. J. and Keyser, D. 1988. Balanced and unbalanced upper-level frontogenesis. *J. Atmos. Sci. 45*, 3366–3386.

Saarikivi, P. and Puhakka, T. 1990. The structure and evolution of a wintertime occluded front. *Tellus 42A*, 122–139.

Sanders, F. 1955. An investigation of the structure and dynamics of an intense surface frontal zone. *J. Meteor. 12*, 542–552.

Sanders, F. and Bosart, L. F. 1985. Mesoscale structure in the megalopolitan snowstorm of 11–12 february 1983. *J. Atmos. Sci. 42*, 1050–1061.

Shapiro, M. A. 1981. Frontogenesis and geostrophically forced secondary circulations in the vicinity of jet stream-frontal zone systems. *J. Atmos. Sci. 38*, 954–973.

Shapiro, M. A., Fedor, L. S. and Hampel, R. 1987. Research aircraft measurements of a polar low over the Norwegian Sea. *Tellus 39A*, 272–306.

Sortais, J. L. 1991. Etude d'un couplage dynamique entre la haute et la basse troposphère: Utilisation du modèle méso-échelle SALSA sur la situation frontale du 11 novembre 1987. Thèse. Université Blaise Pascal, Clermont-Ferrand, France, 270 pp.

Thorpe, A. J. 1990. Frontogenesis at the boundary between air-masses of different potential vorticity. *Q. J. R. Meteorol. Soc. 116*, 561–572.

Uccellini, L. W. and Johnson, D. R. 1979. The coupling of upper and lower tropospheric jet streaks and implications for the development of severe convective storms. *Mon. Wea. Rev. 107*, 682–703.